Repeated CFC sections at the Greenwich Meridian in the Weddell Sea

Olaf Klatt,[1] Wolfgang Roether,[1] Mario Hoppema,[1] Klaus Bulsiewicz,[1] Uli Fleischmann,[1] Christian Rodehacke,[1,2] Eberhard Fahrbach,[3] Ray F. Weiss,[4] and John L. Bullister[5]

Received 21 November 2000; revised 18 June 2001; accepted 13 September 2001; published 25 April 2002.

[1] Repeated observations of the tracer chlorofluorocarbon-11 (CFC-11) for a section along the Greenwich Meridian from Antarctica (70°S) to about 50°S are presented for the period 1984–1998. The CFC sections display a highly persistent pattern. A middepth CFC minimum in the central Weddell Sea is bounded laterally by elevated levels of dissolved CFCs at the southern margin of the Weddell Basin and by a column of elevated CFC concentrations around 55°S near to the northern margin. Part of the latter column covers waters of the Antarctic Circumpolar Current, which indicates that a moderate portion of these waters was ventilated in the Weddell Sea. Deep CFC maxima adjoining the southern and northern margins of the Weddell Basin indicate advective cores of recently ventilated waters. The southern core supports previous notions of deep water import into the Weddell Sea from the east. For all deep and bottom waters, the portions ventilated on the CFC timescale (~50 years) are small. Effective initial CFC saturations for these portions are estimated to be between 60 and 70%, using in part new data from off the Filchner-Ronne Ice Shelf. For various CFC features along the section (mostly advective cores), ventilated fractions and mean ages of these fractions were obtained (with error limits). The procedure was to fit an age distribution of a prescribed form to CFC-11 time series for these features, constructed from the various realizations of the CFC section. The ages are between 3 and 19 years, and the ventilated fractions range between 6 and 23%, indicating a rather limited ventilation of the interior Weddell Sea subsurface layer waters on the CFC timescale. It is shown that the concurrent CFC-12 data provide little additional information. The work demonstrates a high information content of repeated tracer observations and encourages similar approaches also in other ocean regions. *INDEX TERMS:* 4207 Oceanography: General: Arctic and Antarctic oceanography; 4223: Oceanography: General: Descriptive and regional oceanography; 4532 Oceanography: Physical: General circulation; 4294 Oceanography: General: Instruments and techniques

1. Introduction

[2] The bottom waters occupying the major ocean basins are mainly of Antarctic origin and are therefore generically called Antarctic Bottom Water (AABW) [*Wüst*, 1935; *Mantyla and Reid*, 1983]. The Weddell Sea is an important source area of AABW [*Carmack*, 1977; *Foldvik and Gammelsrød*, 1988; *Orsi et al.*, 1999] and thus a key region for the global thermohaline circulation. Weddell Sea waters are largely replenished from Lower Circumpolar Deep Water (LCDW), which, after splitting from the Antarctic Circumpolar Current (ACC) and entering the Weddell Gyre, is commonly called warm deep water (WDW). WDW and surface layer waters derived from it form Weddell Sea Bottom Water (WSBW) but also less dense waters [*Weppernig et al.*, 1996]. Uplifted WSBW, mixing further with WDW, enters the Weddell Sea middepth water column, termed Weddell Sea Deep Water (WSDW), but WSDW also receives input from other sources [*Orsi et al.*, 1993], notably from the east in a southern deep boundary current [*Meredith et al.*, 2000; *Hoppema et al.*, 2001a]. The output of the Weddell Sea to form AABW [*Carmack and Foster*, 1975; *Weiss et al.*, 1979; *Orsi et al.*, 1993] is largely derived from boundary currents adhering to the western and northern slopes of the basin [*Fahrbach et al.*, 1995]. It has been proposed that in recent decades, AABW production has been lower than on the timescale of the global deep water turnover (i.e., several hundred years) [*Broecker et al.*, 1998; 1999], which, if true, would be of considerable climatic relevance. Variability has also been noted on shorter timescales [*Fahrbach et al.*, 2001]. Open ocean convection, which was observed in the 1970s [*Gordon*, 1978], may be a recurrent process of dense water formation. In summary, the modes and rates of turnover and the underlying dynamics, including the aspect of stability of the deep waters in the Weddell Sea and their role in forming AABW, are far from being settled.

[3] A successful methodology to study deep water ventilation and turnover is to utilize observations of anthropogenic, or transient, tracers, such as dissolved chlorofluorocarbons (CFCs) [*Weiss et al.*, 1985; *Bullister*, 1989; *Rhein*, 1991; *Doney and Bullister*, 1992]. The most common CFCs are CFC-11 (CCl_3F) and CFC-12 (CCl_2F_2). The Weddell Sea has been rather extensively monitored for tracers, and the data have been used to study the turnover of the deep waters [e.g., *Weiss et al.*, 1979; *Schlosser et al.*, 1991; *Orsi et al.*, 1999]. *Haine et al.* [1998] treated CFC and CCl_4 data from various sections using a kinematic model to obtain deep water transit times and ventilated portions of the northern deep boundary current that leads into the Indian Ocean.

[1]Institut für Umweltphysik, Universität Bremen, Bremen, Germany.
[2]Also at Max-Planck-Institut für Meteorologie, Hamburg, Germany.
[3]Alfred-Wegener-Institut für Polar- und Meeresforschung, Bremerhaven, Germany.
[4]Scripps Institution of Oceanography, La Jolla, California, USA.
[5]School of Oceanography, University of Washington, Seattle, Washington, USA.

0148-0227/02/2000JC000731

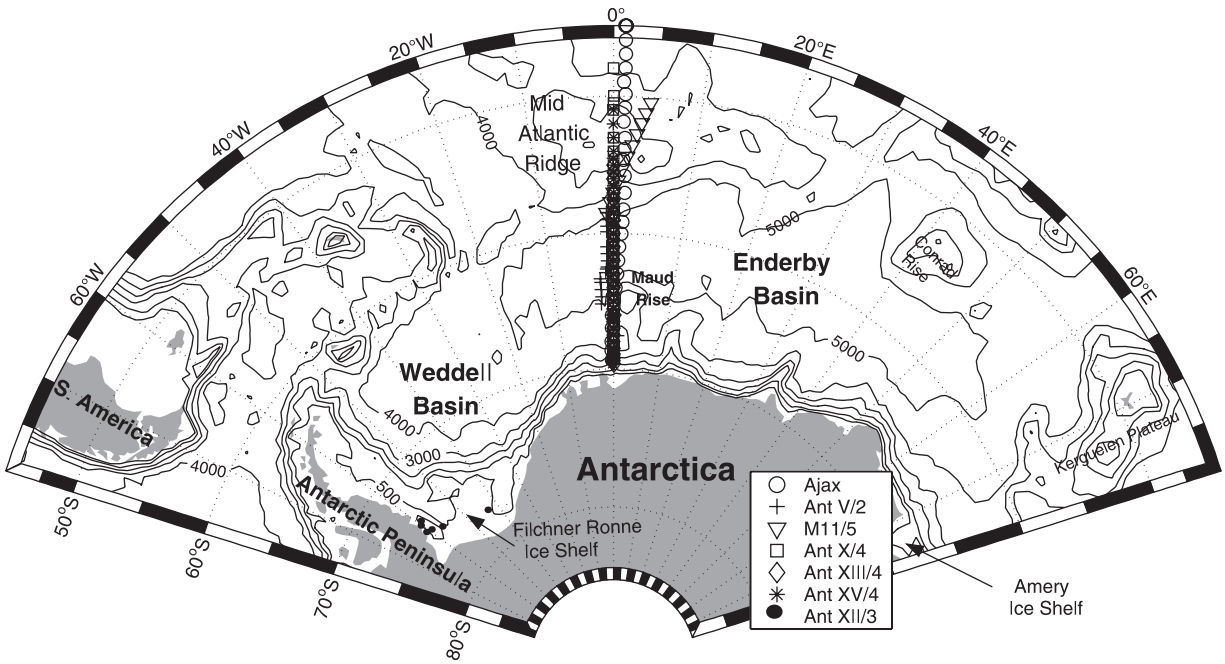

Figure 1. Weddell Sea geography and tracks and stations of sections 1 to 6 (see Table 1) and of cruise ANT XII/3 off the Filchner-Ronne Ice Shelf. Bathymetry is in meters.

A unique situation exists at the Greenwich Meridian in that repeated CFC sections are available, starting with the AJAX project in 1984. The present work analyzes and interprets these sections for the tracer CFC-11. The nature of the information gained is similar to that of *Haine et al.* [1998], but we treat additional features and use a different methodology. Principal results are mean transit times since ventilation and ventilated portions for the features treated.

2. Formation and Turnover of Weddell Sea Waters

[4] LCDW diverted from the ACC enters near to the eastern edge of the Weddell Gyre (20°–30°E), to spread westward as WDW [*Orsi et al.*, 1993; *Hoppema et al.*, 1997]. WDW is characterized by a temperature maximum but becomes gradually cooler and partly upwells into (and mixes with) the surface layer, eventually forming modified WDW (MWDW). The densities of surface waters increase by brine injection during sea ice formation processes particularly on the shelves. Therefore at the southwestern and western margins of the basin, probably up to the tip of the Antarctic Peninsula, these waters attain densities that enable them to sink, entraining MWDW and, partly, also deeper waters [*Carmack and Foster*, 1975; *Foster and Carmack*, 1976; *Foldvik et al.*, 1985; *Gordon et al.*, 1993; *Fahrbach et al.*, 1995]. A principal product is WSBW, which is defined by a potential temperature less than −0.7°C. It appears that the majority of the dense waters generated form a boundary current along the western and northern slopes, which exchanges with the interior waters of the basin only to a limited degree [*Fahrbach et al.*, 1995]. The boundary current feeds exit flows through various gaps in the South Scotia Ridge [*Nowlin and Zenk*, 1988; *Locarnini et al.*, 1993; *Orsi et al.*, 1999], while the deepest part continues eastward to meet the Crozet-Kerguelen Gap at about 55°E [*Haine et al.*, 1998]. Waters deposited close to the bottom of the Weddell Basin can meet these outlets only after having been displaced upwards, whereby they enter the overlying WSDW regime. However, the WSDW range is replenished also from sources farther east, presumably near the Amery Ice Shelf [*Jacobs and Georgi*, 1977], which feed a deep boundary current adjoining the southern continental slope [*Orsi et al.*, 1999; *Meredith et al.*, 2000; *Hoppema et al.*, 2001a]. A special advective feature is the Weddell-Scotia Confluence (WSC), a regime present between the Weddell Sea waters and those of the ACC. The WSC is a shallower feature presumably replenished from the shelf region near to the tip of the Antarctic Peninsula and apparent up to about the Greenwich Meridian [*Muench et al.*, 1990; *Whitworth et al.*, 1994; *Gordon*, 1998]. All these sources add to the formation of AABW. At the Greenwich Meridian the southern boundary of the ACC coincides with the northern boundary of the Weddell Gyre. The boundary is located near 55°S [*Orsi et al.*, 1993; *Schröder and Fahrbach*, 1999], so that LCDW of the ACC and its derivative, WDW, meet in the northern part of the Weddell Basin. The σ_2 = 37.16 kg m^{-3} isopycnal approximately represents their common boundary to WSDW [*Orsi et al.*, 1999], which in the central Weddell Basin roughly corresponds to 1500 m depth. On the southern end of the transect a special circulation pattern is induced by the topographic feature of Maud Rise (Figure 1) [*Gordon and Huber*, 1995; *Muench et al.*, 2001], and the westward coastal current enforces a deepening of the upper layers toward the continental slope.

3. Transient Tracer Situation and Tracer Age Concepts

[5] A fact that makes CFCs particularly suited to study ventilation and turnover timescales in the region is that the WDW is virtually free of CFCs. The LCDW from which the WDW is derived was found to be free of CFCs in Drake Passage in 1990 [*Roether et al.*, 1993] and only limited addition of ventilated waters occurs on the way up to and through the Weddell Sea [*Hoppema et al.*, 2001a]. More elevated concentrations are found in WSBW close to the bottom of the basin and in the cores of newly formed deep waters present on the slopes of the Weddell Basin (see section 4). Their CFC load is predominantly derived from their respective surface layer, or ventilated component (mostly shelf waters; see section 2), which follows the atmospheric CFC trend (Figure 2). However, especially during the cold season, when the surface layer is the densest and therefore apt to form deep and bottom waters, the surface layer CFC concentrations remain markedly below a solubility equilibrium with atmospheric partial pressures. This holds

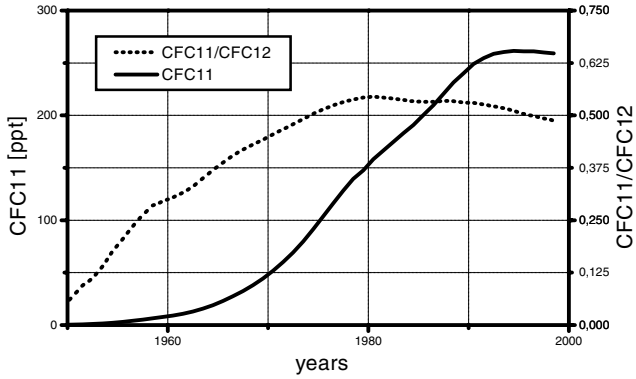

Figure 2. Southern hemisphere atmospheric time history of CFC-11 (ppt) and of the CFC-11/CFC-12 ratio (ppt/ppt) for the period 1950–2000 [*Walker et al.*, 2000]. Corresponding ocean surface layer concentrations are given by (1).

because gas exchange is greatly reduced by ice cover, while at the same time, the surface layer is subject to inflow of low-tracer WDW from below. The resulting CFC saturation is near to 75% over much of the Weddell Sea [*Schlosser et al.*, 1994; *Meredith et al.*, 1996; *Mensch et al.*, 1998a]; but on the shelves from which the ventilated component in deep water formation is primarily drawn, saturation appears to be even lower [*Keir et al.*, 1992]. Off the western shelf, saturations down to ~55% have been observed [*Mensch et al.*, 1998b]. *Roether et al.* [2001] and *Huhn et al.* [2001] discuss effective saturations in newly formed deep waters off the tip of the Antarctic Peninsula, which appear to be similarly low. Since the shelf waters reside on the shelf for some years [*Mensch et al.*, 1996], their apparent undersaturation partly arises from a certain time lag of the mean tracer signature relative to the atmospheric signal (Figure 2), meaning that the degree of undersaturation to some extent depends on (i.e., increases with) the concurrent fractional rate of atmospheric CFC increase.

[6] Given this situation, the CFC data might be evaluated using a model, be it conceptual or dynamical [e.g., *Haine et al.*, 1998; *England and Maier-Reimer*, 2001]. However, in the present work we follow the concept of tracer ages, in which one converts a deep water CFC concentration observed away from the respective formation region into a CFC age (equal to mean transit time since formation). One issue is the dispersion encountered en route from the formation area to the location of observation due primarily to mixing between water parcels that have traveled on trajectories of different transfer times. Therefore one faces a range of transfer times (ages), rather than a fixed one, to the location of observation downstream [*Beining and Roether*, 1996; *Holzer and Hall*, 2000]. From a hypothetical instantaneous tracer spike added to the shelf waters, a delayed, broadened peak would result. Because of a tracer that was advected along trajectories of low speed, the peak should be rather asymmetric with an extended tail, as it is, in fact, found in numerical treatments of the transfer [*Khatiwala et al.*, 2001].

[7] In the Weddell Sea where the deep waters consist of a ventilated, tracer-containing fraction and essentially tracer-free WDW, p_{CFC} ages [*Doney and Bullister*, 1992] make little sense. Such ages are obtained by projecting an observed subsurface CFC concentration (expressed as the equivalent CFC partial pressure in a solubility equilibrium [*Warner and Weiss*, 1985]) on the input time curve (Figure 2) to find an apparent year of descent from the surface layer. The p_{CFC} ages are thus incapable of distinguishing between a tracer-containing and a tracer-free portion. More appropriate would be the use of tracer ratio ages. Such ages yield (1) a mean age for the tracer containing (young) component of the water and (2) the fractional contribution of this component. The remainder of the water is taken to be tracer-free, effecting a dilution of the tracer concentrations [*Weiss et al.*, 1985]. A time-invariant circulation is assumed, and the procedure is to adjust the mixture of young water and tracer-free water to match the input time histories of both tracers (Figure 2). However, the classical CFC-11 to CFC-12 ratios ages have a limited dynamic range, in particular, in the presence of strong mixing, and since about 1980 they are subject to age ambiguity [*Beining and Roether*, 1996]. In fact, we show in section 6 that for our data set CFC-11 to CFC-12 ratio ages are hardly meaningful.

[8] An approach complementary to tracer ratio dating is enabled by the repeated CFC observations that we have available, which similarly allow constraining ages and fractional contributions of the young-water component. Repeated observations might suffer from insufficient comparability at (essentially) the same location but will provide information on presence or absence of prominent changes in the hydrography and/or circulation. An advantage is that the degrees of freedom, basically the number of repeats, exceed the just two from a single observation of two tracers. In section 6 we exploit this to obtain error estimates. The way in which we account for the mentioned age dispersion en route is also outlined in section 6.

4. Data

[9] We use tracer and hydrographic data collected on six (sections 1–6) along the Prime Meridian between Antarctica (70°S) and approximately 50°S, spanning the period from 1984 to 1998. A listing of the data sets is given in Table 1. Station positions on these expeditions are shown in Figure 1. The tracks differ slightly, in particular for sections 1 to section 3, while the later ones exactly follow the Greenwich Meridian. Only three sections, i.e., section 1, section 4, and section 6, extend over the full range in latitude (~70°–50°S), while section 2 and section 5 range from 70° to 58°S and 70° to 55°S, respectively, and section 3 only goes from 57° to 51°S. Cruise 1 was part of the AJAX expeditions, cruise 2 was part of the Winter Weddell Sea Project 1986 (WWSP86), and cruises 3 to 6 were part of the World Ocean Circulation Experiment (WOCE) program. Note that cruises 2 and 4 were austral winter cruises, while the others were carried out in late summer or fall. However, we presume seasonality to be of little relevance to the deep tracer fields at the Greenwich Meridian because of the distance from water mass source regions. Furthermore, we present data of POLARSTERN cruise ANT XII/3, 1995 [*Jokat and Oerter*, 1997], from stations on the deep shelf adjoining the Filchner-Ronne Ice Shelf.

[10] Samples for the measurement of transient tracers were collected using conventional conductivity-temperature-depth rosette systems equipped with standard Niskin bottles. Water samples for CFC analysis were drawn using glass syringes on all cruises except for section 5 and section 6, which used flow-through glass ampoule containers [*Bulsiewicz et al.*, 1998]; for section 5 a

Table 1. List of Expeditions

Section	Expedition	Dates	Vessel	Cruise Report
1	AJAX Leg 2	11 Jan. to 19 Feb. 1984	R/V *Knorr*	[*SIO and TAMU*, 1985]
2	ANT V/2	27 Jun. to 11 Jul. 1986	R/V *Polarstern*	[*Schnack-Schiel*, 1987]
3	M11/5	23 Jan. to 5 Mar. 1990	R/V *Meteor*	[*Roether et al.*, 1990]
4	ANT X/4	21 May to 5 Aug. 1992	R/V *Polarstern*	[*Lemke*, 1994]
5	ANT XIII/4	17 Mar. to 20 May 1996	R/V *Polarstern*	[*Fahrbach and Gerdes*, 1997]
6	ANT XV/4	28 Mar. to 23 May 1998	R/V *Polarstern*	[*Fahrbach*, 1999]

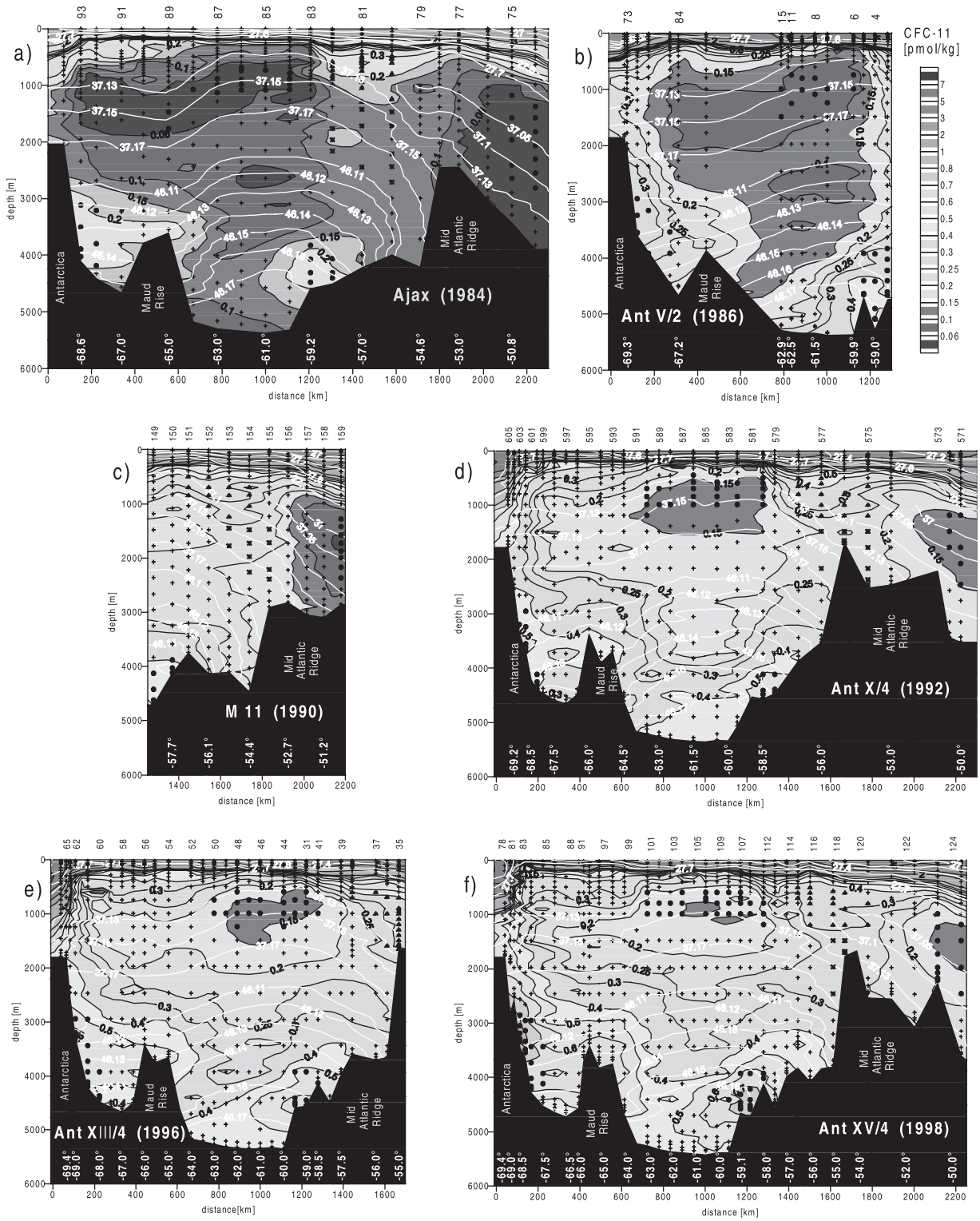

Figure 3. CFC-11 sections at the Prime Meridian, Antarctica to ~50°S: (a) AJAX, 1984; (b) ANT V/2, 1986; (c) M 11/5, 1990; (d) ANT X/4, 1992; (e) ANT XIII/4, 1996; and (f) ANT XV/4, 1998. The color scale is identical for all sections, isolines are shown for 0.06, 0.1, 0.15, 0.2, 0.25, 0.3, 0.4,. . .0.8, 1, 2, 3, 5, and 7 pmol kg^{-1}. Isopycnals (white lines) are in σ_0, σ_2, and σ_4, down to 1000 m, 3000 m, and bottom, respectively (density contouring is based on bottle data only). Dots indicate data, station numbers are shown at the top, and latitude is shown at the bottom. The data points taken to obtain the core concentrations listed in Table 2 are marked (southern and northern deep core with dots, Lower Circumpolar Deep Water of Antarctic Circumpolar Current (ACC) with triangles, midsection CFC saddle point with crosses, Weddell Sea and ACC CFC minimum with dots). The sections differ slightly (Figure 1), the distance is along-track, and the scale is always starting at 70°S on the Prime Meridian. See color version of this figure at back of this issue.

small correction for sample degassing in the ampoule containers had to be applied. All CFC measurements have been carried out using a purge and trap gas chromatographic system with an electron capture detector. For the cruises up to 1990 (1 to 3) a packed column technique was used [*Bullister and Weiss*, 1988] (for cruise 3, see the report by *Roether et al.* [1993]) and, later on, a capillary-column technique [*Bulsiewicz et al.*, 1998]. The analytical columns were a DB-624 on section 4, a combination of a DB-VRX and a short carbograph packed column on section 5, and, because of a breakdown of the packed column, a DB-VRX column only on section 6. The CFC data for sections 1 and 2 are available in the form of data reports [*Weiss et al.*, 1990; *Huber et al.*, 1989]. These data were published previously [e.g., *Mensch et al.*, 1996; *Haine et al.*, 1998; *Orsi et al.*, 1999]. All later CFC data have been submitted to the related WOCE center, while only parts have so far been published (sections 3 and 4 [*Sültenfuss*, 1998]). CFC measurements on ANT XII/3 were made at Bremen using the same capillary column technique on samples stored in flame-sealed glass ampoules [*Bulsiewicz et al.*, 1998]. Herein we primarily address the CFC-11 data, but CFC-12 data are also available for all sections. There are, furthermore, CFC-113 and CCl_4 data for one of the later realizations of the section each, but these are ignored for the sake of a more uniform approach in the present work.

[11] The precision of the CFC-11 measurements in the case of cruises 1 and 2 was 1% or 0.005 pmol kg^{-1} (whichever is greater), 2% or 0.01 pmol kg^{-1} in the case of cruise 3, 1.4% or 0.006 pmol kg^{-1} in the case of 4, and 1.0% or 0.004 pmol kg^{-1} for cruises 5 and 6. Machine blanks were generally low, and sample blanks were either determined from measurements of supposedly CFC-free waters or estimated from variability of the lowest concentrations observed. Precisions for the ANT XII/3 measurements are similar, but there is an additional uncertainty due to the sample storage, which, according to measurements at sea and in the laboratory made on concurrent samples from various cruises, are lower than 3% for CFC-12 for the concentration range in question and a little larger (< 4%) for CFC-11. Data are reported on the Scripps Institution of Oceanography 1993 scale (SIO 93). Part of the data were originally calibrated to the SIO 1986 scale, but have been converted to SIO 93 by dividing the CFC-11 concentrations by 1.0251. Water densities were calculated from the bottle data sets for all sections (for temperature and salinity accuracies, see *Scripps Institution of Oceanography and Texas A&M University* [1985] (SIO and TAMU) and *Fahrbach et al.* [2001]; accordingly, densities used herein should be accurate to better than ±0.005 kg m^{-3}).

5. Tracer Sections

[12] CFC-11 sections for all six realizations are presented in Figure 3. A continuous increase in concentrations with time is evident throughout the water column. The CFC-11 increase from 1984 to 1998 is approximately threefold in the deeper waters in comparison with a 40% increase of the atmospheric partial pressure during this period (Figure 2). The rates of increase become smaller toward the surface, and at the surface itself the concentrations even fail to increase between 1996 and 1998, following the atmospheric forcing. All sections are characterized by a rather shallow surface layer of high concentrations, which contrasts with far lower concentrations in the deeper waters, amounting to at most ~10% of those at the surface. The depths of this layer vary, partly in response to depth changes of the related isopycnals. The layer is thus shallowest over the central Weddell Sea (approximately 59°–64°S) and reaches the deepest at the far ends of the section, strongly so toward the southern continental slope, and more moderately, intersecting isopycnals, north of about 51°S in the Cape Basin. There are two middepth CFC minima, which characterize the water ventilated the slowest. One minimum is located in the Weddell Sea at about 600 to 1800 m depth. It is centered at approximately σ_2 = 37.15 kg m^{-3}, i.e., within the WDW but rather close to the WDW-WSDW boundary (section 2). The other minimum, displaying similarly low concentrations, is found toward the northern end of the section, at a somewhat greater depth and near to σ_2 = 37.00 kg m^{-3}. The minima are separated by a vertical column of coherently higher concentrations slightly south of the Mid-Atlantic Ridge (MAR) at approximately 53°–59°S. The upper part of this column is centered near the southern ACC boundary (at ~55°S, see section 2) and is thus partly made up of ACC waters. A similar column of elevated CFC concentrations is present adjoining the southern slope. The concentrations here exceed those of the midsection column, and a relative CFC minimum is indicated at 1800–2000 m depth.

[13] The mentioned southern slope and midsection columns of enhanced CFC concentrations follow the topography and lead downward into deep CFC cores adjoining the southern and northern slopes of the Weddell Basin. The southern deep core extends beyond Maud Rise, while in between the cores the middepth tracer minimum extends downward. The two cores represent the mentioned southern inflow and northern outflow of the western Weddell Sea. The inflow is centered at about 69°S at depths between 2200 m and 4300 m. The outflow is located at the base of the slope of the MAR at about 59°S between 3800 m and 4800 m depth. The densities in the centers of the two cores are different, approximately σ_4 = 46.12–46.13 kg m^{-3} for the southern core and 46.16 kg m^{-3} for the northern one, while their CFC concentrations are rather similar. We note that cruise ANT V/2 (section 2) stands out in that concentrations in the deep core adjoining the MAR appear to increase down to 5000 m. However, we ascribe this to the fact that the section is farther west compared with the other sections and shows a different bottom topography. Apart from this, the general deep CFC pattern is persistent between the sections. The density field also appears to be quite invariant. An exception is a moderate drift in density (increase during 1984–1998 of ~0.01 kg m^{-3}) below about 3000 m depth in the southern half of the Weddell Sea, probably related to gradual changes in of temperature and salinity of WDW and WSBW during this period [*Fahrbach and Gerdes*, 1997].

[14] There are, of course, differences in detail between the CFC realizations beyond the mentioned general temporal trend (i.e., a threefold increase during 1984–1998), although these have to be interpreted with care considering the spatial resolution and contouring of the data. These differences include the following: (1) Concentrations in the midsection vertical column of enhanced concentrations below the surface layer just south of the MAR (~56°S) appear to increase rather more gradually. (2) At midbasin (~62°S), concentrations at the bottom possibly increase a little less with time than those near 3000 m depth. (3) There is quite a noticeable change in the form of the northern boundary of the Weddell Sea middepth tracer minimum, from being rather vertical in the beginning to being more inclined (i.e., leaning northward) later. (4) The Weddell Basin tracer minimum appears to be filled in a little faster in the south. (5) The southward jump in concentrations at ~500 m depth changes in latitude, from near 66°S early on to ~64°S later; this change is particularly noticeable in relation to the σ = 37.13 kg m^{-3} isopycnal.

6. Analysis of CFC Time Series

[15] The temporal development of the CFC concentrations according to Figure 3 was analyzed for the following advective cores, or CFC extrema: (1) the deep southern inflow core of elevated CFC concentrations at the slope of the Antarctic continent (67°–70°S, 3000–4500 m depth; marked data points (dots) in Figure 3), (2) the deep northern outflow core adjoining the MAR (58°–61°S, 4000–4500 m), (3) the plateau of higher concentrations within the midsection vertical column of enhanced CFC concentrations representing LCDW just north of the southern ACC boundary (approximately 56°S, 600 m), (4) the CFC saddle

Table 2. Time Series of CFC-11 Concentrations (pmol kg^{-1}) in Various Deep Cores Along the Greenwich Meridian (See Text)[a]

Section	Location	1984 (Number of Observations[b])	1986 (Number of Observations[b])	1990 (Number of Observations[b])	1992 (Number of Observations[b])	1996 (Number of Observations[b])	1998 (Number of Observations[b])
1	Southern deep core	0.23 ± 0.01 (7)	0.31 ± 0.03 (9)	ND	0.48 ± 0.02 (10)	0.55 ± 0.01 (14)	0.73 ± 0.02 (19)
2	Northern deep core	0.22 ± 0.01 (7)	0.40 ± 0.02 (16)	0.46 ± 0.02 (7)	0.56 ± 0.02 (7)	0.68 ± 0.02 (8)	0.72 ± 0.02 (15)
3	LCDW of ACC	0.21 ± 0.01 (19)	ND	0.31 ± 0.02 (15)	0.32 ± 0.01 (18)	0.34 ± 0.01 (20)	0.33 ± 0.01 (22)
4	Midsection CFC saddle point	0.14 ± 0.01 (11)	ND	0.22 ± 0.01 (10)	0.22 ± 0.01 (10)	0.27 ± 0.02 (8)	0.29 ± 0.01 (6)
5	Weddell Sea CFC minimum	0.05 ± 0.01 (18)	0.08 ± 0.01 (12)	ND	0.14 ± 0.01 (24)	0.15 ± 0.01(21)	0.17 ± 0.01 (29)
6	ACC CFC minimum	0.04 ± 0.01 (13)	ND	0.07 ± 0.01 (8)	0.13 ± 0.01 (7)	ND	0.16 ± 0.01 (12)

[a] Errors are standard errors of the mean values based on the apparent scatter of the individual data on which the average values are based. ND denotes no data.
[b] These are numbers on which the concentrations are based; the observations used are also marked in Figure 3.

point below this plateau (approximately 55°S, 2000 m), (5) the Weddell Sea middepth tracer minimum (59°–69°S, 800–1800 m), and (6) the deep CFC minimum in the northern part of the ACC (north of 52°S, about 1500 m). The results of this procedure, including estimated errors (based on data spread), are listed in Table 2, and the time series for all cores are shown in Figure 4. The temporal increases are roughly linear, with the exception of core 3. The increase for this core, which is the shallowest one, is far more gradual. In fact, the time series at 3 resembles more the atmospheric input time curve (Figure 2), although this resemblance might be a coincidental result of temporal changes in the effective ventilation of this core.

[16] We proceed by constructing a transfer function from the atmospheric partial pressures (Figure 2) to the time series of Table 2. A time-invariant circulation is assumed (see section 7), but, opposed to *Haine et al.* [1998], we do not account for circulation and mixing in any explicit way. Instead, we consider that whatever the circulation field, the result will be a spread in the year of descent of this component from the surface layer (see section 3), which we account for in the form of an age distribution of the tracer-containing component. In this way we avoid a need to specify effects like a net loss of tracer from a core, or an entrainment of essentially tracer-free water into it, and we are enabled to treat the CFC extrema 3–6 in Table 2, for which the renewal mechanism would be difficult to specify. Only to obtain a closed analytical form, we approximate the age spread by an age distribution that formally corresponds to tracer propagation under one-dimensional advection-diffusion (mean along-core velocity u and apparent diffusivity κ) [*Kreft and Zuber*, 1978]. The distribution is illustrated in Figure 5. For a low age spread it is essentially Gaussian, while for a higher spread it shows the desired feature of a tail toward high ages (section 3). The distribution is of a form $n(t, \tau, \sigma)$ (for functional form, see (2)), where t is the subsurface transit time (or age), τ is the mean age, and σ is a characteristic age spread (years). The parameters τ and σ are related to the formal transport parameters by $\tau = l/u$ (l = distance from formation location) and $\sigma^2 = 2\kappa\tau u^{-2}$, a Peclet number being $Pe = ul/\kappa = 2\tau^2/\sigma^2$.

[17] The CFC concentration of a water parcel as it descends from the surface layer (shelf waters) at time t_{desc}, $c_0(t_{\mathrm{desc}})$, is taken to be

$$c_0(t_{\mathrm{desc}}) = \xi c_{\mathrm{eq}}(t_{\mathrm{desc}}) = \xi f(T,S) P_{\mathrm{atm}}(t_{\mathrm{desc}}), \qquad (1)$$

where c_{eq} is the concentration in equilibrium with the atmospheric partial pressure P_{atm} (Figure 2), $f(T, S)$ is the CFC solubility function [*Warner and Weiss*, 1985] (T is temperature, S is salinity), and ξ ($0 \le \xi \le 1$) is the apparent degree of saturation of the

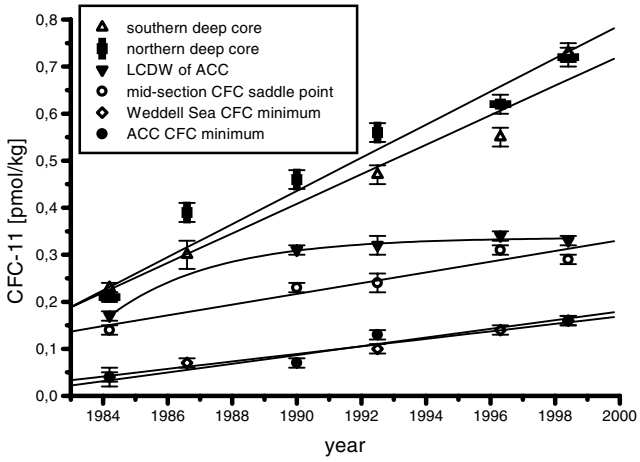

Figure 4. CFC-11 time series (pmol kg^{-1}) in cores 1–6. Error bars are standard errors, see Table 2. Curves connecting the data points are drawn by eye.

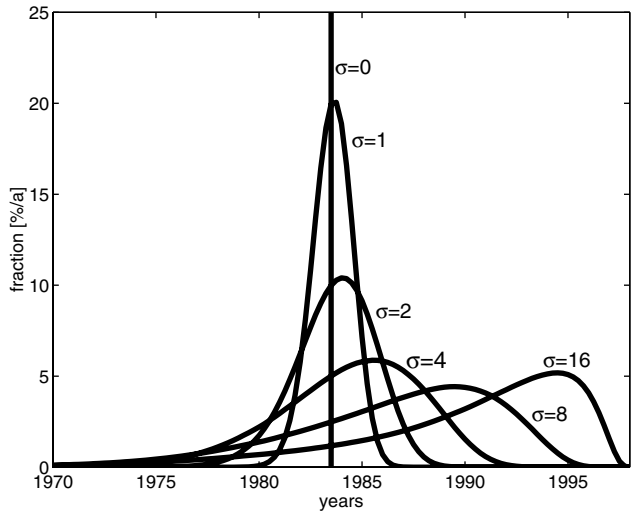

Figure 5. Age distribution $n(t, \tau, \sigma)$ (norm $\{n\}$ is unity; t is age, τ is mean age, σ is spread parameter) used in evaluating the CFC time series of Table 2 and Figure 4 for different values of σ (years), see text. The distribution is that for tracer propagation under one-dimensional advection-diffusion [*Kreft and Zuber*, 1978]. The plot is for a mean age of 15 years, which is typical of the Weddell Sea (Table 3), and for observation in 1998.

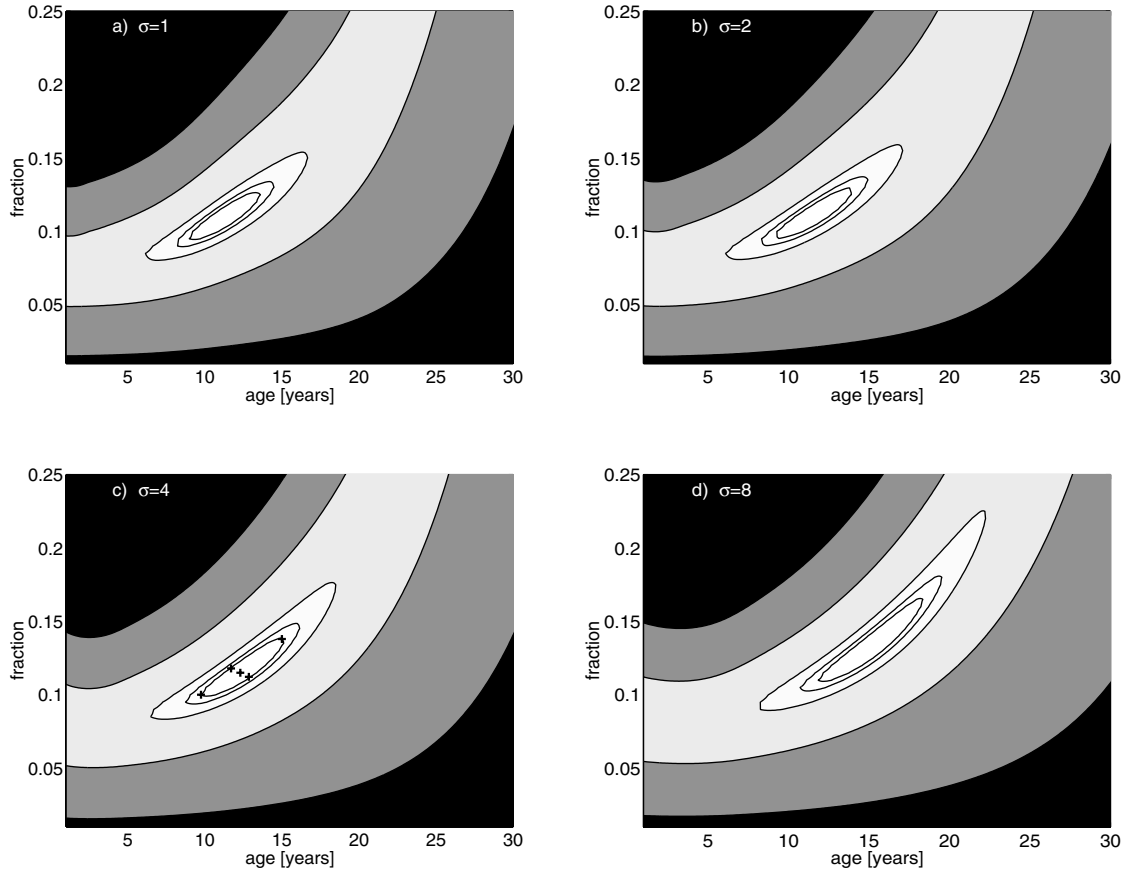

Figure 6. Variance isolines in a plot fraction of the tracer-containing component, $\gamma\xi$, versus mean age, τ (years), of this component for the southern deep core, for σ = (a) 1, (b) 2, (c) 4, and (d) 8 years. The isolines correspond to 30, 50, 100, 500, and 1000% excess over the minimum variance (Table 3). In Figure 6c (σ = 4 years) the location of the minimum variance and four locations on the innermost variance isoline are indicated. Time curves according to (2) for these $\gamma\xi$ and τ pairs are given in Figure 7.

descending water, which we assume to be invariant in time (cf. section 3). Note that ξ implicitly accounts for any aging during residence on the shelf and the related age dispersion; the "clock" thus starts only when the waters leave the surface layer. Concentrations at any given subsurface location at time t_{obs}, $c(t_{obs})$, are taken to correspond to a mixture of (1) old, CFC-free waters effecting a dilution γ, and (2), younger waters that descended from the surface layer over a certain range of time prior to t_{obs} (distributed in time as shown in Figure 5), carrying CFC concentrations according to (1). Using $t_{desc} = t_{obs} - t$ (t is age in years), the relationship between $c(t_{obs})$ and $c_{eq}(t_{obs} - t)$ is given by

$$c(t_{obs}) = \gamma\xi \int_0^\infty n(t,\tau,\sigma)\, c_{eq}(t_{obs} - t)\, dt$$
$$= \gamma\xi \int_0^\infty \sqrt{\frac{\tau^3}{2\pi\sigma^2 t^3}} \exp\left[\frac{(t-\tau)^2\tau}{2\sigma^2 t}\right] c_{eq}(t_{obs} - t)\, dt\,. \qquad (2)$$

The free parameters in (2), i.e., τ, σ, and the product $\gamma\xi$, are determined using the time series $c_{obs}(t^i_{obs})$ for the cores in question (Table 2); thereafter, γ is separated by choosing a value for ξ (equation (1)). However, since low significance was found when all three parameters were determined jointly, the procedure in practice was to do repeated determinations of τ and $\gamma\xi$ with a prescribed σ, varying the latter parameter over a reasonable range. We are thus unable to determine σ, but we do learn to which extent the values of the other parameters depend on the degree of age dispersion. This means that the nature of our results remains similar to those of tracer ratio dating, except that we consider age dispersion explicitly and address confidence limits beyond those due to measurement errors, as is outlined next.

[18] A least mean square approach was applied, minimizing the difference between the observed concentrations, c_{obs}, and the corresponding ones according to (2) in the form of

$$S \equiv \frac{1}{(N-2)} \sum_{i=1}^{N} \frac{1}{\delta_{obs}(t^i_{obs})^2} \left[c_{obs}(t^i_{obs}) - c(t^i_{obs})\right]^2, \qquad (3)$$

where N is the number of observations for each core. The degrees of freedom are reduced by 2 to account for the determination of the two parameters τ and $\gamma\xi$, and the concentration difference is scaled by the uncertainty $\delta_{obs}(t^i_{obs})$ (Table 2) of the respective observational value $c_{obs}(t^i_{obs})$. It follows that if this uncertainty were the only source of error, the expectation value of the variance S would become unity. A value exceeding unity will thus indicate a contribution of other sources of error (assumed form of the age distribution, deviations from a steady state, etc.).

[19] As an example of the results in detail, Figure 6 shows variance isolines for the southern deep core, on a parameter plane tracer-saturated fraction, $\gamma\xi$, versus mean age, τ, of this component, for a number of values of the age spread σ. One notes that the variance isolines form a slightly curved valley, such that a larger mean age is correlated with a larger tracer-saturated fraction. The

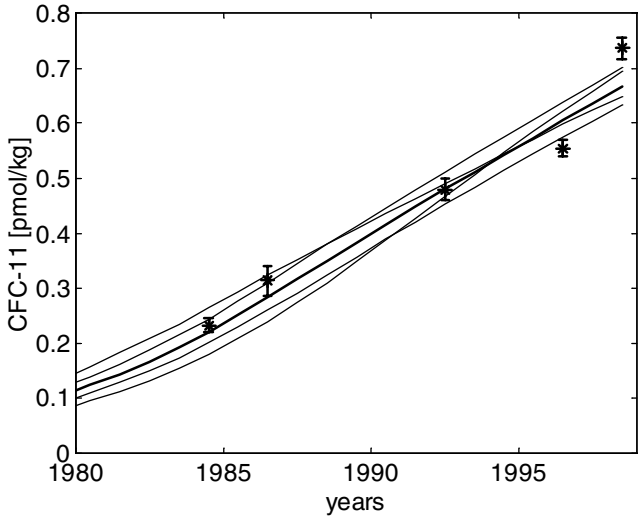

Figure 7. Reconstructed CFC time curves (pmol kg^{-1}) according to (2) for the southern deep core for σ = 4 years and for the parameter values in Table 3 (bold curve) and four parameter locations marked in Figure 6c on the innermost variance isoline (thin curves), in comparison with the observations, marked by asterisks with error bars (Table 2).

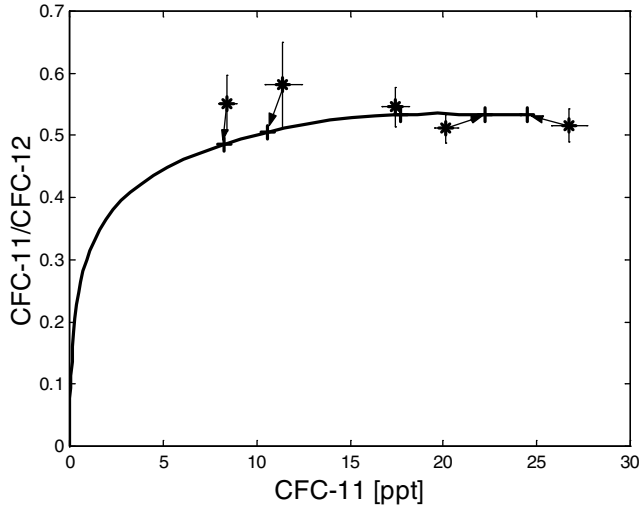

Figure 8. CFC-11/CFC-12 ratio (ppt/ppt) versus CFC-11 partial pressure (ppt) in the southern deep CFC core as a function of time, according to (2) (curve), and to the observations (data points; from AJAX, 1984 (left) up to ANT XV/4, 1998 (right); Table 2). Arrows connect the data points with the locations on the curve for the same period (straight crosses). Errors are 1-Sigma errors of the mean accounting for the apparent scatter of the data on which the respective data points are based.

explanation is that a larger mean age implies lower CFC concentrations (Figure 2), so that a larger CFC-saturated fraction is required to reproduce an observed concentration. For a similar reason, fraction and mean age both increase with σ, but markedly so only above σ = 4 years. In the plot for σ = 4 years (Figure 6c), the locations of the minimum variance and the four locations on the innermost variance isoline are marked. Figure 7 shows the degree to which (2), with the parameter sets corresponding to these locations, reproduces the observations. One finds that the observations are compatible with the envelope of the concentration-versus-time curves for these parameter sets. A similar correspondence also holds for the other time series (not shown). We conclude that the variance isoline in question (variance 30% above minimum value) approximately defines 1-sigma uncertainty ranges for the governing parameters (i.e., fraction and mean age of the CFC-saturated component).

[20] Table 3 lists the resulting mean ages and fractions of the tracer-saturated component for all time series of Table 2, together with estimated uncertainties, assuming age spreads of σ = 4 years for series 1–4 and 8 years for 5 and 6. The rationale for this choice is that the former are advective cores, for which an 8-year time spread is regarded as rather high (Figure 5), whereas the latter time series are for locations believed to be replenished largely by mixing and thus are subject to a distinctly higher age spread. The uncertainties listed are the respective full parameter spreads corresponding to a 30% increase in variance above the minimum value (innermost isoline in Figure 6); that is, they ignore the potential constraint from their mentioned interdependence. The errors are moderate, except for the mean age of core 3 (LCDW of southern ACC). We repeat that, if the age spreads were indeed distinctly higher than assumed, the data of Table 3 would underestimate both the mean ages and tracer-saturated fractions; age spreads lower than assumed, on the other hand, would produce only a small decrease (see Figure 6). The "Slope" column in Table 3, furthermore, lists the slopes fraction versus age, $\partial(\gamma\xi)/\partial\tau$, at the variance minimum, to characterize the interdependence of the parameters. The average value of the minimum variance (sixth column in Table 3) is approximately unity, so that there is no hint beyond that

Table 3. Mean Age (τ, years) and Fraction ($\gamma\xi$,%) of the CFC-Saturated Water Component, Related Interdependence (Slope $\partial(\gamma\xi)/\partial\tau$, % yr^{-1}), and Value of the Variance Minimum (Equation (3)), for the Time Series of Table 2, See Text[a]

Section	Location	Mean Age[b], Years	CFC Saturated Fraction[b], %	Slope, %/*a*	Minimum Variance	Assumed Saturation[b,c], %	Ventilation Fraction[b,c], %
1	Southern deep core	12.5 ± 2.5	12 ± 2	0.8	1.0	60 ± 5	20 ± 3
2	Northern deep core	13.5 ± 2.5	14 ± 3	1.0	1.0	60 ± 5	23 ± 5
3	LCDW of ACC	3 ± 3	5.5 ± 0.5	0.1	0.3	70 ± 5	8 ± 1
4	Midsection CFC saddlepoint	8.5 ± 1	4.7 ± 0.5	0.2	0.3	65 ± 5	7 ± 1
5	Weddell Sea CFC minimum	17 ± 4	4 ± 1	0.3	2.0	60 ± 5	7 ± 1
6	ACC CFC minimum	19 ± 3	4.5 ± 1	0.5	0.9	70 ± 5	6 ± 1

[a] For the first four cores, the values are for σ = 4 years, and for the last two (Weddell and ACC minima) they are for σ = 8 years.
[b] Uncertainties are estimated standard errors.
[c] The assumed apparent saturations and the resulting ventilated fractions are of the surface layer waters in the respective formation areas, see section 7.

Table 4. Mean CFC-12 and CFC-11 Concentrations (pmol kg^{-1}) and Resulting Apparent Saturations (%) on the Deep Shelf Off the Filchner-Ronne Ice Shelf (Cruise ANT XII/3, 1995) 300 m to Bottom[a]

	Number of Data Points	Mean Concentration[b]	Saturation[b]
CFC-11	23	4.82 ± 0.03	61 ± 1
CFC-12	24	2.10 ± 0.01	56 ± 1

[a] All samples were approximately at freezing temperature. For station positions, see Figure 1.

[b] Errors are 1-sigma error of the mean, accounting for data spread only.

of the observational uncertainties (equation (3)). We mention in passing that the data of Table 3 formally correspond to Peclet numbers ranging between 1 and 23.

[21] Figure 8, finally, addresses the potential value of the additional CFC-12 data available. Shown is a time curve of the CFC-11/CFC-12 ratio versus the CFC-11 partial pressure according to (2) for the southern deep core (Table 3) in comparison with the available observations. Evidently, the curve is compatible with the observations, lending support to our theoretical approach. However, any more detailed conclusions are impossible owing to the considerable uncertainties in the observed CFC-11 to CFC-12 ratios. For example, changes in the form of the curve when the age spread σ is varied by a factor of 2 (not shown) remain small compared with these uncertainties. The problem is that, while between 1984 and 1998 the partial pressures rose threefold, the change in the ratios according to the curve has been no larger than ~10% (after 1990, 1% change only). The uniformity of the ratios presumably is due to prominent mixing between waters of different age [*Beining and Roether*, 1996]. Such uniformity also shows up in plots like in Figure 8 of the entire subsurface layer data of any one of the realizations of the section (not shown). This even holds for the AJAX section data, which represent the earliest observations in the set and should thus be influenced the least by the ambiguity due to the atmospheric ratio maximum that occurred in about 1980 (Figure 2). The only useful piece of information is that for a given CFC-11 partial pressure the observed ratios are distinctly higher than those in the atmosphere and, rather, correspond to those of far younger waters. A strong dilution by CFC-free water is thus indicated. Beyond this, the general conclusion is that CFC-12 hardly provides any additional age information.

7. Discussion

[22] In section 5 we noted a high persistency in structure among the various CFC-11 sections (Figure 3), which is remarkable considering that the sections span a time interval of as much as 14 years. This finding adds to the general notion in the literature of missing evidence of fundamental changes in the deep circulation of the Weddell Sea. The CFC observations are incompatible with major changes, such as, for example, onset of the deep southern inflow only after the beginning of the observations, or substantial breaks in the rates and densities of the deep waters formed. Because of (advective) delay between the actual occurrences of any changes upstream, and their appearance at the Greenwich Meridian section, the period will be shifted back in time by a few years relative to the observation period (1984–1998), the degree of delay being related to the mean ages and age dispersions of Table 3. Absence of major changes in circulation and ventilation, in turn, implies that the observations can be taken to represent a time-averaged situation. We therefore conclude that the analysis of the CFC data in the section 6 is justified and that the results in Table 3 relate to mean values over a period as just circumscribed. However, it must be realized that this conclusion does not exclude even a considerable interannual variability of the ventilation (concerning the rates and properties of the waters formed) and the circulation of the deep waters because the CFC signatures represent a time-integrated information (as shown by (2), for example). On the other hand, the differences between the various realizations of the CFC section noted in section 5 are not necessarily positive evidence of such variations, because the transfer function from surface water tracer concentrations to those at depth is by no means uniform in space. This means that even in a time-invariant situation the actual form of the concentration increase with time will vary with location.

[23] According to Table 3 the mean ages of all cores are rather moderate (<20 years), and the fractions of CFC-saturated water are quite small (<15%). The mean age is the lowest for the upper part of the midsection column of enhanced CFC concentrations (core 3, LCDW of southern ACC), where at the same time the CFC-saturated fraction is particularly low. The highest ages, but, similarly, low CFC-saturated fractions, are found for the Weddell Basin and ACC CFC minima. Both the southern and northern deep cores have intermediate ages and comparatively high saturated fractions, which are, in fact, quite similar for the two cores.

[24] Of special oceanographic interest is the ventilated fraction, γ, i.e., the fraction of the water acquired from the surface layer. To obtain it, the CFC-saturated fraction ($\gamma\xi$ in (2), Table 3) must be split into γ and the effective initial saturation of this component, ξ. As noted in section 3, the winter surface layer everywhere in the Weddell Sea shows an undersaturation of at least about 25%, yielding $\xi = 0.75$ as an upper limit. Table 4 lists CFC-11 and CFC-12 saturations observed on the deep shelf in front of the Filchner-Ronne Ice Shelf during Polarstern cruise ANT XII/3 (1995). The bottom depth was approximately 600 m and the average below 300 m is listed. The data show little scatter (error of the mean <1%). For CFC-12, the data of which are relatively more accurate (section 3), the saturation including the mentioned 3% concentration uncertainty due to the sample storage is 56 ± 2%. The expected corresponding CFC-11 saturation (scaling the saturation deficit by $Sc^{-0.5}$, where Sc is Schmidt number [*Zheng et al.*, 1998]) is 58 ± 2%, which is compatible with the measured average CFC-11 saturation (61 ± 1%). The data thus point to an effective CFC-11 saturation for the ventilated waters from the Filchner-Ronne Ice Shelf region of $\xi = 0.58 \pm 0.02$. This value is consistent with the 55% saturation reported by *Mensch et al.* [1998b] off the western shelf south of 65°S, 53°W; they find higher saturations farther north (up to 85%), but these observations at the same time were made farther off the shelf break. We make the assumption that the ANT XII/3 saturations are typical for the northern deep core and that similarly low saturations hold for the source regions of the southern deep core [see *Keir et al.*, 1992], while saturations for waters formed farther north along the Antarctic Peninsula are somewhat higher. Rounded saturations ξ for all cores, with tentative uncertainties, were chosen on this basis (Table 3, "Assumed Saturation" column). Note that the actual choice is not too critical, since the total range mentioned (58–75%) is rather moderate. The resulting ventilated fractions (rightmost column in Table 3) are quite small, i.e., 6–7%, for the CFC minima and for the midsection middepth water column (cores 3–6), and approximately 20% for the deep southern and northern cores. We repeat, however, that the saturations of Table 3 (seventh column) ignore the mentioned dependence of ξ on the rates of atmospheric CFC increase during the respective ventilation periods (section 3). Considering that the observational evidence rests on measurements made during the 1990s, the saturations of Table 3 might be high by a moderate factor, which means that the ventilated fractions would be underestimated by the same factor. We believe that the effect could amount at most to ~20%.

[25] Our estimated transit time and ventilated fraction for the northern deep core (13.5 ± 2.5 years; 23 ± 5%; Table 3) are close to, and consistent with, values reported by *Haine et al.* [1998] (12 ± 4 years; 12–25%). Such agreement is particularly gratifying, as the observational basis and methodology employed are quite different. The values for the southern core have been used to estimate the ventilation rate due to this core [*Hoppema et al.*, 2001a], which was found to be considerable. We believe that at most a limited part of this core is incorporated directly into the high-CFC core at the western margin of the basin. The reason is that the latter core forms a thin sheet extended over more or less the entire western continental slope [cf. *Hoppema et al.*, 2001a, Figure 2], while the southern deep core at the Greenwich Meridian is rather wide in comparison and restricted in depth (Figure 3). Therefore the southern core presumably largely replenishes the interior WSDW, to feed the WSDW upwelling, but possibly also to become entrained gradually into the deep boundary current at the western and northern slopes (section 2).

[26] The small ventilated fraction of the CFC minimum core in the Weddell Sea indicates that there is little replenishment of the inner deep waters of the Weddell Sea on the CFC timescale. A rough estimate of the overall renewal timescale at the minimum is obtained by assuming the renewal of 7% within 17 years (as by Table 3) to be valid uniformly, yielding a renewal time by ventilated waters of 240 years (i.e., 17/0.07 = 243). Such a long renewal time implies that, for example, a significant amount of anthropogenic CO_2 will show up in the minimum core with great delay [*Hoppema et al.*, 2001b]. Even considering that a recirculation among the deep waters may be distinctly faster, the present results support the notion that much of the new deep waters formed leave the basin without much mixing with the interior waters [*Fahrbach et al.*, 1995; *Orsi et al.*, 1999]. Ignoring this fact has led to underestimating the renewal times of the deep waters at large [*Jenkins et al.*, 1983; *Mensch et al.*, 1996]. A rather lower deep water renewal time was also hinted by *Schlosser et al.* [1994], who considered their estimate of 125 years based on ^{39}Ar data as too high.

[27] The deep southern and northern cores have similar mean ages and ventilated fractions, while the water density for the former core is distinctly less (Figure 3). This excludes a substantial contribution of recirculated northern core waters to the southern core, in keeping with *Haine et al.* [1998]. If there were indeed such a contribution, it would have had to lose density to a considerable degree by mixing with less dense waters above it, which would induce a CFC loss since the waters available for admixture have distinctly lower CFC concentrations (Figure 3). Recirculated northern core waters subjected to such mixing would thus hardly add to the CFC-saturated fraction in the southern core. Considering a scheme that the Weddell Gyre consists of two subgyres [*Beckmann et al.*, 1999], on the other hand, there might be a contribution of the southern core to the midsection column of enhanced concentrations, if such waters follow an internal recirculation to the west of the Greenwich Meridian. However, such a trajectory would have to pass through the tracer minimum present at latitudes in between (Figure 3), which means that a subdivision of the gyre presumably is restricted to the upper waters.

[28] Features of particular interest are the elevated concentrations in several hundred meters depth above the MAR, i.e., within the LCDW of the southern ACC (core 3 in Table 3). Since, as mentioned, such water was found to be tracer-free in Drake Passage in 1990 [*Roether et al.*, 1993], the feature supports the notion that the LCDW in question has a contribution of waters ventilated in the Weddell Sea [*Orsi et al.*, 1999]. The low age suggests that the source area is not too far away, probably near to the tip of the Antarctic Peninsula, i.e., related to the WSC [*Muench et al.*, 1990; *Whitworth et al.*, 1994]. A similar source area is likely for the CFC saddle point (core 4 in Table 3), which also has a low age. The small ventilated fractions of both cores mean that dilution has been particularly strong. This can be ascribed to mixing promoted by the high current velocities of the ACC and the steep topography below the features. Mesoscale ACC meandering may cause a certain variability of the LCDW core, possibly explaining the mentioned larger age uncertainty for this core. Although the CFC concentrations in the LCDW in question are moderate (Table 2), the source strength of the corresponding Weddell Sea component may still be considerable in view of the large volumes of water moved by the ACC.

[29] The reported Weddell Sea open-ocean convection in the 1970s, which took place not far west of the Greenwich Meridian section [*Gordon*, 1978], should have transferred tracer into the low-CFC deep waters. However, we cannot identify any signature in our data that could be attributed to the convective event(s). The middepth tracer minimum layer was, in fact, particularly well developed in our earliest observations (1984, Figure 3a), i.e., those nearest to the event(s). The concentrations in the minimum layer are quite small, so that sizable contributions of surface layer waters should have made a distinct effect. The missing signature thus means that the signature was either advected away before 1984, or that the convective event(s) was (were) of limited significance.

8. Conclusions

[30] Our observations represent a series of snapshots of the CFC concentrations at a Greenwich Meridian section, spanning more than a decade (1984–1998). They provide a vivid illustration of the evolving oceanic CFC transient in the presence of a rather stable density field (Figure 3). The CFC pattern between the various realizations of the section is highly persistent. This persistency means that for a period beginning in about 1980, i.e., a period shifted a few years back relative to the observation period, fundamental changes in the ventilation and circulation of the subsurface waters along the section were absent. The data do not provide information on interannual or shorter timescales because the nature of the CFC signature, and mixing upstream of the section, largely filter out the effects of such variations. The CFC pattern supports the notion of a substantial deep water import into the Weddell Sea from sources to the east in form of a deep flow along the southern margin of the Weddell Basin [*Orsi et al.*, 1999; *Meredith et al.*, 2000; *Hoppema et al.*, 2001a]. It is, furthermore, evident that the ACC receives ventilated waters from the Weddell Sea area [*Orsi et al.*, 1999]. The CFC pattern does not show any signature of open-ocean convective events [*Gordon*, 1978].

[31] The repeated CFC realizations were used to derive ventilated fractions and mean ages of these fractions (with estimated errors) for six subsurface cores (mostly CFC extrema) along the section (Table 3) in a new fashion (section 6). The ventilated fractions range between 6 and 23%, and their mean ages range between 3 and 19 years. According to these values, there is only a very moderate renewal of the Weddell Sea deep waters on the CFC timescale (section 7). The new method uses a parameter fitting to CFC time series for the various cores for all realizations and an age distribution (Figure 5) rather than a fixed mean age of the tracer-containing fraction. The age distribution chosen is an approximation, but this is deemed acceptable since the age distribution is primarily used to determine to which extent the derived mean ages and ventilated fractions depend on the degree of age dispersion. The initial CFC saturation of the ventilated fraction, which is required to determine this fraction, was estimated using in part new CFC data from the deep shelf off the Filchner-Ronne Ice Shelf, taken in 1995 (Table 4). It was concluded that the ventilated portion of the subsurface waters from this source carries a CFC-11 saturation of only ~60%. However, the saturation prior to the 1990s might have been even somewhat lower, and hence the

ventilated fraction might be a little higher than deduced (Table 3). This issue should be addressed in future work. It was shown that the classical CFC-11/CFC-12 ratio dating is hardly applicable in the waters in question (Figure 8). Further evaluation of the data of Table 3 is left to future work.

[32] It will be most desirable to repeat the Greenwich Meridian CFC section in the future, and judging from Figure 5, an adequate repetition period should be about 5 years. Such repeats will extend in time the monitoring of any fundamental changes in ventilation and circulation of the Weddell Sea. Furthermore, unless such changes are found, added future realizations of the section will allow refined ventilation estimates for the subsurface waters. Atmospheric CFC concentrations have begun to decrease in recent years (Figure 2), but the deep water CFC concentrations will continue to be far lower than those of surface layer waters. The reversal of the atmospheric CFC time trend, in fact, should cause the temporal development of the deep water CFC concentrations (Figure 4) to depend on age dispersion more than under the steadier atmospheric trend that has prevailed previously. However, the initial CFC saturations of the ventilated fractions will likewise be affected, so that an adequate quantification of these saturations will be a prerequisite for exploiting the effect.

[33] If, like in our case, several repeated CFC observations are available, the new approach is statistically superior to traditional tracer dating, such as CFC-11/CFC-12 dating from a single cruise (section 3). We not only obtained mean ages and ventilated fractions of the waters in question but also uncertainty limits for these quantities. Such information goes clearly beyond the one that can be gained from traditional tracer ratio dating based on data from a single cruise (section 3). We encourage application of the new method also in other ocean regions for which repeated transient tracer observations are available. Most useful will be observations spanning a decade or more, so that the concentration increase in the deep waters can sufficiently exceed effects of hydrographic variability, and the number of repeats should amount to at least three so that uncertainty estimates are enabled. Additional age information could be gained by including further tracers, such as CFC-113 and CCl_4. It is hoped that the present work may contribute to a continued use of tracer-based ages as a valid alternative to using tracer observations in models directly.

[34] **Acknowledgments.** We are grateful to the masters and crew of the various cruises from which our data originate and to numerous helpers at sea and in the laboratory. We thank M. P. Schodlok, Bremerhaven, for discussions. Cruises METEOR M 11/5 and POLARSTERN ANT XV/4 were supported by the Deutsche Forschungsgemeinschaft, and ANT X/4, XII/3, and XIII/4, as well as much of the CFC measurements, were supported by the Bundesminister für Forschung und Technologie (grants Fkz 03F0538A, Fkz 03F0050B, Fkz 03F010121A, and Fkz 03F0157A), both institutions at Bonn-Bad Godesberg, Germany. Further support was provided by the Environment and Climate Programme of the European Union under grant ENV4-CT97-0472, and by the Dutch-German cooperative program NEBROC. We greatly appreciate the comments of three anonymous reviewers, which helped us to shape the final manuscript.

References

Beckmann, A., H. H. Hellmer, and R. Timmermann, A numerical model of the Weddell Sea: Large-scale circulation and water mass distribution, *J. Geophys. Res.*, *104*, 23,375–23,391, 1999.

Beining, P., and W. Roether, Temporal evolution of CFC-11 and CFC-12 concentrations in the ocean interior, *J. Geophys. Res.*, *101*, 16,455–16,464, 1996.

Broecker, W. S., S. L. Peacock, S. Walker, R. Weiss, E. Fahrbach, M. Schröder, U. Mikolajewicz, R. Key, T.-H. Peng, and S. Rubin, How much deep water is formed in the Southern Ocean?, *J. Geophys. Res.*, *103*, 15,833–15,843, 1998.

Broecker, W. S., S. Sutherland, and T.-H. Peng, A possible 20th-century slowdown of Southern Ocean deep water formation, *Science*, *286*, 1132–1135, 1999.

Bullister, J. L., Chlorofluorocarbons as time-dependent tracers in the ocean, *Oceanography*, 12–17, 1989.

Bullister, J. L., and R. F. Weiss, Determination of CCl_3F and CCl_2F_2 in seawater and air, *Deep Sea Res.*, *35*, 839–853, 1988.

Bulsiewicz, K., H. Rose, O. Klatt, A. Putzka, and W. Roether, A capillary-column chromatographic system for efficient chlorofluorocarbon measurement in ocean waters, *J. Geophys. Res.*, *103*, 15,959–15,970, 1998.

Carmack, E. D., Water characteristic of the Southern Ocean south of the Polar front, in *A Voyage of Discovery*, edited by M. Angel, pp. 15–43, Pergamon, Tarrytown, New York, 1977.

Carmack, E. D., and T. D. Foster, On the flow of water out of the Weddell Sea, *Deep Sea Res.*, *22*, 711–724, 1975.

Doney, S. C., and J. L. Bullister, A chlorofluorocarbon section in the eastern North Atlantic, *Deep Sea Res.*, *39*, 1857–1881, 1992.

England, M. H., and E. Maier-Reimer, Using chemical tracers to assess ocean models, *Rev. Geophys.*, *39*, 29–70, 2001.

Fahrbach, E. (Ed.), Die Expedition ANTARKTIS XV/4 des Forschungsschiffes "Polarstern" 1998 (The Expedition ANTARKTIS of the Research Vessel "Polarstern" in 1998), in *Ber. Polarforsch. 314,* 109 pp., Alfred-Wegener-Inst. für Polarforsch., Bremerhaven, Germany, 1999.

Fahrbach, E., and D. Gerdes (Eds.), Die Expedition ANTARKTIS XIII/4-5 des Forschungsschiffes "Polarstern" 1996 (The Expedition ANTARKTIS XIII/4-5 of the Research Vessel "Polarstern" in 1996), *Ber. Polarforsch. 239*, 106 pp., Alfred-Wegener-Inst. für Polarforsch., Bremerhaven, Germany, 1997.

Fahrbach, E., G. Rohardt, N. Scheele, M. Schröder, V. Strass, and A. Wisotzki, Formation and discharge of deep and bottom water in the northwestern Weddell Sea, *J. Mar. Res.*, *53*, 515–538, 1995.

Fahrbach, E., S. Harms, G. Rohardt, M. Schröder, and R. A. Woodgate, Flow of bottom water in the northwestern Weddell Sea, *J. Geophys. Res.*, *106*, 2761–2778, 2001.

Foldvik, A., and T. Gammelsrød, Notes on Southern Ocean hydrography, sea-ice and bottom water formation, *Palaeogeogr. Palaeoclimatol. Palaeoecol.*, *67*, 3–17, 1988.

Foldvik, A., T. Gammelsrød, and T. Toressen, Circulation and water masses on the southern Weddell Sea shelf, in *Oceanology of the Antarctic Continental Shelf*, *Antarct Res. Ser.*, vol. 43, edited by S. S. Jacobs, pp. 5–20, AGU, Washington, D. C., 1985.

Foster, T. D., and E. D. Carmack, Frontal zone mixing and Antarctic Bottom Water formation in the southern Weddell Sea, *Deep Sea Res.*, *23*, 301–317, 1976.

Gordon, A. L., Deep Antarctic convection west of Maud Rise, *J. Phys. Oceanogr.*, *8*, 600–612, 1978.

Gordon, A. L., Western Weddell Sea thermohaline stratification, in *Ocean, Ice and Atmosphere: Interactions at the Antarctic Continental Margin*, *Antarct. Res. Ser.*, vol. 75, edited by S. S. Jacobs and R. F. Weiss, pp. 215–240, AGU, Washington, D. C., 1998.

Gordon, A. L., and B. A. Huber, Warm Weddell Water west of Maud Rise, *J. Geophys. Res.*, *100*, 13,747–13,753, 1995.

Gordon, A. L., B. A. Huber, H. H. Hellmer, and A. Ffield, Deep and bottom water of the Weddell Sea's western rim, *Science*, *262*, 95–97, 1993.

Haine, T. W. N., A. J. Watson, M. I. Liddicoat, and R. R. Dickson, The flow of Antarctic bottom water to the southwest Indian ocean estimated using CFCs, *J. Geophys. Res.*, *103*, 27,637–27,653, 1998.

Holzer, M., and T. M. Hall, Transit-time and tracer-age distribution in geophysical flows, *J. Atmos. Sci.*, *57*, 3539–3558, 2000.

Hoppema, M., E. Fahrbach, and M. Schröder, On the total carbon dioxide and oxygen signature of the Circumpolar Deep Water in the Weddell Gyre, *Oceanol. Acta*, *20*, 783–798, 1997.

Hoppema, M., O. Klatt, W. Roether, E. Fahrbach, K. Bulsiewicz, C. Rodehacke, and G. Rohardt, Prominent renewal of Weddell Sea Deep Water from a remote source, *J. Mar. Res.*, *59*, 257–279, 2001a.

Hoppema, M., W. Roether, R. G. J. Bellerby, and H. L. W. de Baar, Direct measurements reveal insignificant storage of anthropogenic CO_2 in the abyssal Weddell Sea, *Geophys. Res. Lett.*, *28*, 1747–1750, 2001b.

Huber, B. A., P. A. Mele, W. E. Haines, A. L. Gordon, J. C. Jennings, L. I. Gordon, R. F. Weis, F. A. Van Woy, and P. K. Salameh, CTD and hydrographic data from cruise ANT V/2 of R/V Polarstern, *Tech. Rep. LDGO-89-3*, Lamont-Doherty Geol. Obs., Palisades, New York, 1989.

Huhn, O., W. Roether, P. Beining, and H. Rose, Validity limits of carbon tetrachloride as an ocean tracer, *Deep Sea Res., Part I*, *48*, 2025–2049, 2001.

Jacobs, S. S., and D. T. Georgi, Observations on the southwest Indian/Antarctic Ocean, in *A Voyage of Discovery*, edited by M. Angel, pp. 43–85, Pergamon, New York, 1977.

Jenkins, W. J., D. E. Lott, M. W. Pratt, and R. D. Boudreau, Anthropogenic tritium in South Atlantic bottom water, *Nature*, *305*, 45–46, 1983.

Jokat, W., and H. Oerter (Eds.), Die Expedition ANTARKTIS-XII mit FS "Polarstern" 1995: Bericht vom Fahrtabschnitt ANT-XII/3 (The Expedi-

tion ANTARKTIS-XII of RV "Polarstern" in 1995: Report of Leg ANT-XII/3), in *Ber. Polarforsch. 219*, 188 pp., Alfred-Wegener-Inst. für Polarforsch., Bremerhaven, 1997.

Keir, R. S., R. L. Michel, and R. F. Weiss, Ocean mixing versus gas exchange in Antarctic shelf waters near 150°E, *Deep Sea Res.*, *39*, 97–119, 1992.

Khatiwala, S., M. Visbeck, and P. Schlosser, Age tracers in an ocean GCM, *Deep Sea Res., Part I*, *48*, 1423–1441, 2001.

Kreft, A., and A. Zuber, On the physical meaning of the dispersion equation and its solutions for different initial and boundary conditions, *Chem. Eng. Sci.*, *33*, 1471–1480, 1978.

Lemke, P. (Ed.), Die Expedition ANTARKTIS X/4 des FS "Polarstern" 1992 (The Expedition ANTARKTIS X/4 of the RV "Polarstern" in 1992), in *Ber. Polarforsc. 140*, 90 pp., Alfred-Wegener-Inst. für Polarforsch., Bremerhaven, Germany, 1994.

Locarnini, R. A., T. Whitworth III, and W. D. Nowlin Jr., The importance of the Scotia Sea on the outflow of Weddell Sea Deep Water, *J. Mar. Res.*, *51*, 135–153, 1993.

Mantyla, A. W., and J. L. Reid, Abyssal characteristics of the world ocean waters, *Deep Sea Res., Part A*, *30*, 805–833, 1983.

Mensch, M., R. Bayer, J. L. Bullister, P. Schlosser, and R. F. Weiss, The distribution of tritium and CFCs in the Weddell Sea during the mid-1980s, *Progr. Oceanogr.*, *38*, 377–415, 1996.

Mensch, M., A. Simon, and R. Bayer, Tritium and CFC input functions for the Weddell Sea, *J. Geophys. Res.*, *103*, 15,923–15,937, 1998a.

Mensch, M., W. M. Smethie, P. Schlosser, R. Weppernig, and R. Bayer, Transient tracer observations from the western Weddell Sea during the drift and recover of Ice Station Weddell, in *Ocean, Ice, and Atmosphere: Interactions at the Antarctic Continental Margin*, *Antarct. Res. Ser.*, vol. 75, edited by S. S. Jacobs and R. F. Weiss, pp. 241–256, AGU, Washington, D. C., 1998b.

Meredith, M. P., K. A. van Scoy, A. Watson, and R. A. Locarnini, On the use of carbon tetrachloride as a transient tracer of Weddell Sea deep and bottom waters, *Geophys. Res. Lett.*, *23*, 2943–2946, 1996.

Meredith, M. P., R. A. Locarnini, K. A. V. Scoy, A. J. Watson, K. J. Heywood, and B. A. King, On the sources of Weddell Gyre Antarctic Bottom Water, *J. Geophys. Res.*, *105*, 1093–1104, 2000.

Muench, R. D., J. T. Gunn, and D. M. Husby, The Weddell-Scotia Confluence in midwinter, *J. Geophys. Res.*, *95*, 18,177–18,190, 1990.

Muench, R. D., J. H. Morison, D. Martinson, P. Schlosser, B. Huber, and R. Hohmann, Maud Rise revisited, *J. Geophys. Res.*, *106*, 2423–2440, 2001.

Nowlin, W. D. Jr., and W. Zenk, Westward bottom currents along the margin of the south Shetland island arc, *Deep Sea Res.*, *35*, 269–301, 1988.

Orsi, A. H., W. D. Nowlin Jr., and T. Whitworth III, On the circulation and stratification of the Weddell Gyre, *Deep Sea Res.*, *40*, 169–203, 1993.

Orsi, A. H., G. C. Johnson, and J. L. Bullister, Circulation, mixing and production of Antarctic Bottom Water, *Prog. Oceanogr.*, *43*, 55–109, 1999.

Rhein, M., Ventilation rates of the Greenland and Norwegian Seas derived from distributions of the chlorofluoromethanes F11 and F12, *Deep Sea Res., Part A*, *38*, 485–503, 1991.

Roether, W., M. Sarnthein, T. J. Müller, W. Nellen, and D. Sahrhage, Südatlantik — Zirkumpolarstrom, Reise Nr. 11, 3. Oktober 1989-11. März 1990, *Meteor Ber. 90-2*, 169 pp., Inst. für Meereskunde Hamburg, Hamburg, Germany, 1990.

Roether, W., R. Schlitzer, A. Putzka, P. Beining, K. Bulsiewicz, G. Rohardt, and F. Delahoyde, A chlorofluoromethane and hydrographic section across Drake Passage: Deep water ventilation and meridional property transport, *J. Geophys. Res.*, *98*, 14,423–14,435, 1993.

Roether, W., B. Klein, and K. Bulsiewicz, Apparent loss of CFC-113 in the upper ocean, *J. Geophys. Res.*, *106*, 2679–2688, 2001.

Schlosser, P., J. L. Bullister, and R. Bayer, Studies of deep water formation and circulation in the Weddell Sea using natural and anthropogenic tracers, *Mar. Chem.*, *35*, 97–122, 1991.

Schlosser, P., B. Kromer, R. Weppernig, H. H. Loosli, R. Bayer, G. Bonani, and M. Suter, The distribution of ^{14}C and ^{39}Ar in the Weddell Sea, *J. Geophys. Res.*, *99*, 10,275–10,287, 1994.

Schnack-Schiel, S. (Ed.), Die Winter — Expedition mit FS "Polarstern" in die Antarktis (ANT V/1–3) (The winter expedition of R/V "Polarstern" to the Antarctic (ANT V/1–3)), in *Ber. Polarforsch. 39*, 259 pp., Alfred-Wegener-Inst. für Polarforsch., Bremerhaven, Germany, 1987.

Schröder, M., and E. Fahrbach, On the structure and the transport of the eastern Weddell Gyre, *Deep Sea Res., Part II*, *46*, 501–527, 1999.

Scripps Institution of Oceanography and Texas A&M University (SIO and TAMU), Physical, chemical and in-situ CTD data from the AJAX expedition in the South Atlantic, 275 pp., Scripps Inst. of Oceanogr., La Jolla, Calif., 1985.

Sültenfuss, J., Das Radionuklid Tritium im Ozean: Meßverfahren und Verteilung von Tritium im Südatlantik und im Weddellmeer, *Ber. Polarforsch. 256*, 200 pp., Alfred-Wegener-Inst. für Polar- und Meeresforsch., Bremerhaven, Germany, 1998.

Walker, S. J., R. F. Weiss, and P. K. Salameh, Reconstructed histories of annual mean atmospheric mole fraction for the halocarbons CFC-11, CFC-12, CFC-113, and carbon tetrachloride, *J. Geophys. Res.*, *105*, 14,285–14,296, 2000.

Warner, M. J., and R. F. Weiss, Solubilities of chlorofluoromethanes 11 and 12 in water and seawater, *Deep Sea Res.*, *32*, 1485–1497, 1985.

Weiss, R. F., H. G. Östlund, and H. Craig, Geochemical studies of the Weddell Sea, *Deep Sea Res., Part A*, *26*, 1093–1120, 1979.

Weiss, R. F., J. L. Bullister, R. H. Gammon, and M. J. Warner, Atmospheric chlorofluoromethanes in the deep equatorial Atlantic, *Nature*, *314*, 608–610, 1985.

Weiss, R. F., J. L. Bullister, M. J. Warner, F. A. van Woy, and P. K. Salameh, AJAX Expedition Chlorofluorocarbon Measurements, 190 pp., Scripps Inst. of Oceanogr., La Jolla, Calif., 1990.

Weppernig, R., P. Schlosser, S. Khatiwala, and R. G. Fairbanks, Isotope data from Ice Station Weddell: Implications for deep water formation in the Weddell Sea, *J. Geophys. Res.*, *101*, 25,723–25,739, 1996.

Whitworth, T. III, W. D. Nowlin Jr., A. H. Orsi, R. A. Locarnini, and S. G. Smith, Weddell Sea shelf water in the Bransfield Strait and Weddell-Scotia Confluence, *Deep Sea Res.*, *41*, 629–641, 1994.

Wüst, G., Schichtung und Zirkulation des Atlantischen Ozeans: Das Bodenwasser und die Stratosphäre, *Wiss. Ergeb. Dtsch. Atl. Meteor 1925–1927*, *6*, 288, 1935.

Zheng, M., W. J. De Bruyn, and E. S. Saltzman, Measurements of the diffusion coefficients of CFC-11 and CFC-12 in pure water and seawater, *J. Geophys. Res.*, *103*, 1375–1379, 1998.

J. L. Bullister, NOAA/PMEL, 7600 Sand Point Way N.E., Seattle, WA 98115, USA. (John.L.Bullister@noaa.gov)

K. Bulsiewicz, U. Fleischmann, M. Hoppema, O. Klatt, C. Rodehacke, and W. Roether, Institut für Umweltphysik, Universität Bremen, P.O. Box 330 440, D-28334 Bremen, Germany. (oklatt@physik.uni-bremen.de)

E. Fahrbach, Alfred-Wegener-Institut für Polar- und Meeresforschung, P.O. Box 120161, Bremerhaven, D-27515 Germany.

R. F. Weiss, Scripps Institution of Oceanography, University of California, 447 Endurance Hall, 8675 Discovery Way, La Jolla, CA 92093, USA. (rfweiss@ucsd.edu)

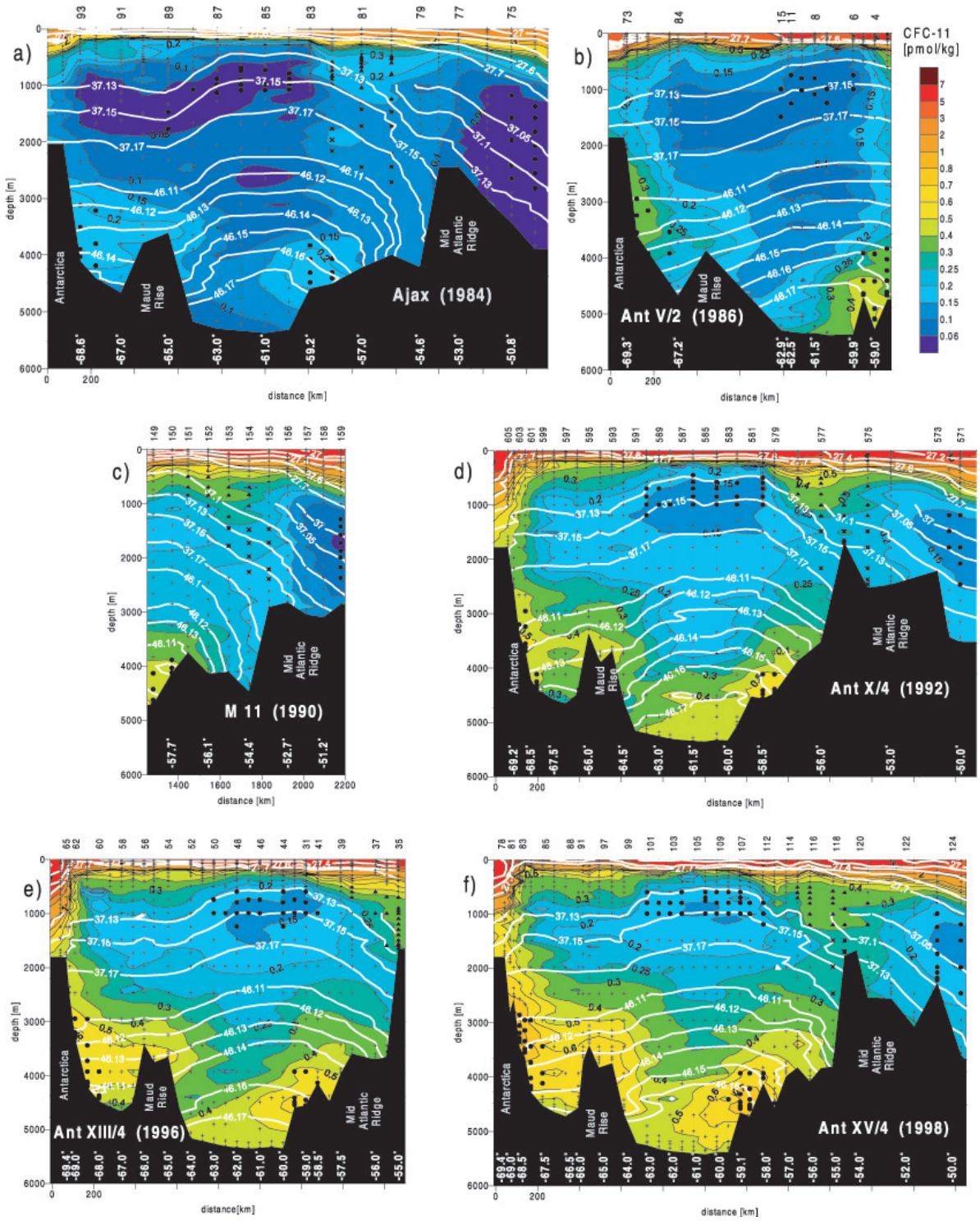

Figure 3. CFC-11 sections at the Prime Meridian, Antarctica to ~50°S: (a) AJAX, 1984; (b) ANT V/2, 1986; (c) M 11/5, 1990; (d) ANT X/4, 1992; (e) ANT XIII/4, 1996; and (f) ANT XV/4, 1998. The color scale is identical for all sections, isolines are shown for 0.06, 0.1, 0.15, 0.2, 0.25, 0.3, 0.4,. . .0.8, 1, 2, 3, 5, and 7 pmol kg^{-1}. Isopycnals (white lines) are in σ_0, σ_2, and σ_4, down to 1000 m, 3000 m, and bottom, respectively (density contouring is based on bottle data only). Dots indicate data, station numbers are shown at the top, and latitude is shown at the bottom. The data points taken to obtain the core concentrations listed in Table 2 are marked (southern and northern deep core with dots, Lower Circumpolar Deep Water of Antarctic Circumpolar Current (ACC) with triangles, midsection CFC saddle point with crosses, Weddell Sea and ACC CFC minimum with dots). The sections differ slightly (Figure 1), the distance is along-track, and the scale is always starting at 70°S on the Prime Meridian.